Data-Driven Multiobjective Optimization of Wave-Packets for Near-Field Subsonic Jet Noise

Giorgio Palma, Stefano Meloni, Roberto Camussi, Umberto Iemma, Christophe Bogey

A data-driven multi-objective optimization of wave–packets for near–field subsonic jet noise

Giorgio Palma*
Roma Tre University, Via Vito Volterra, 62, 00146 Roma, RM, Italy

Stefano Meloni,†
University of Tuscia, 01100 Viterbo, VT, Italy

Roberto Camussi,‡, Umberto Iemma,§
Roma Tre University, Via Vito Volterra, 62, 00146 Roma, RM, Italy

Christophe Bogey¶
Fluid Mechanics and Acoustics Laboratory, LMFA, UMR 5509, Ecully, 69130, France

Aeroacoustics of innovative aircraft cannot disregard the development of low-order models for the jet noise source, which are essential to assess the propulsion-airframe interactions from the conceptual design stage. The main scope of this work is to provide a noise source model that can be coupled with relatively low computational cost methods for aeroacoustic scattering. To this end, this paper presents for the first time a multi-objective optimization of the 0^{th} mode wave–packet in the jet near-field. The importance of calibrating the model with near-field pressure data stems from the fact that in new aircraft the engine nacelles are typically positioned at a few diameters from the wing or fuselage. In this work, the near-field of a high-subsonic jet at a Mach number of 0.9 is represented as a cylindrical surface radiating the pressure disturbances of a wave–packet source, optimized using large-eddy simulation data from three lines at different radial distances. The optimized model has been tested at Strouhal numbers up to 1, and the optimized solutions have been chosen using a Pareto-ranking criterion which considers the wave–packet prediction over an extra line. A good agreement is achieved between the reference data and model predictions, for multiple near-field radial distances.

*Post–Doc Research Fellow, Department of Engineering, Corresponding Author, giorgio.palma@uniroma3.it, AIAA Member

†Assistant Professor, Department of Economics, Engineering, Society and Business Organization, Corresponding Author, stefano.meloni@unitus.it, AIAA Member

‡Full Professor, Department of Engineering, roberto.camussi@uniroma3.it

§Full Professor, Department of Engineering, umberto.iemma@uniroma3.it, Associate Fellow AIAA

¶CNRS Research Scientist, Univ Lyon, Central School of Lyon (ECL), INSA Lyon, Univ Claude Bernard Lyon I, christophe.bogey@ec-lyon.fr, Associate Fellow AIAA

Presented as Paper AIAA 2022-2934 at the 28th AIAA/CEAS Aeroacoustics 2022 Conference, Southampton, UK, June 14-17, 2022;

Nomenclature

x, r, θ	=	cylindrical coordinates
c_∞	=	speed of sound of the unperturbed flow
D	=	nozzle exhaust diameter
p	=	pressure
f	=	frequency
ω	=	$2\pi f$ angular frequency in radians
k	=	ω/c_∞ acoustic wave–number
Re_D	=	$\rho U D/\mu$ nozzle exhaust Reynolds number
He_l	=	kl Helmholtz number with characteristic lenght l
St_D	=	fD/U Strouhal number
U_j	=	nozzle exhaust jet velocity
M	=	U_j/c_∞ jet Mach number
δ_{BL}	=	nozzle exhaust boundary layer
J	=	objective function
$\mathbf{q}$	=	parameters vector
$\mathbf{v}$	=	design variables vector
TI	=	Turbulence Intensity
SPL	=	Sound Pressure Level

I. Introduction

Since the beginning of aeroacoustics, jet noise has been considered a hot topic in aviation noise because of its dominant role in community exposure. The incoming of increasingly strict noise regulations makes essential the development of modern strategies to reduce the noise emitted by jets and aircraft engines. The design of a modern commercial aircraft must consider the acoustic emissions from the early conceptual phase, hence reliable and fast prediction methods are of fundamental importance. Tremendous efforts have been and are being deployed in the development of more effective acoustic treatments and devices for quieter aviation, such as quieter high lift devices [1], chevrons for jet exhaust [2, 3], acoustic liners, and/or innovative treatments [4–8] for turbofans ducts. Innovative configurations are being studied to avoid technological saturation in the race for aviation noise abatement. Blended and Hybrid Wing Body (BWB) aircraft is probably the most promising alternative to the currently dominating tube-and-wing configuration, both in terms of efficiency and community noise reduction [9–12]. The main characteristic of a BWB is the non-net distinction between the fuselage occupying the center body and wings, with the former being wider

and shaped like an airfoil to provide a non-negligible contribution to the overall lift, resulting in a sensible efficiency increase. The large center body surface offers the possibility of the upper installation of the propulsion system, which can be exploited for the acoustic shielding of the engine noise [13–15]. The simulation of the shielding effect in the audible frequency range involves the solution of the scattering problem of the whole aircraft up to extremely high Helmholtz number $He_l = kl$, with k the wave–number and l a characteristic length of the aircraft, *e.g.* the center body length, which makes it computationally very expensive in particular when introduced in an optimization process. There is, hence, a strong need for fast models for predicting the effects of the propulsion system installation on the acoustic emissions at the aircraft level, enabling its assessment from the first design stages and also for disruptive configurations. Adaptive metamodeling techniques have been recently applied to this class of problems[16, 17] to reduce the computational effort required in determining the optimal position of the propulsion system that minimises the noise directed towards the ground and community. Boundary Elements Method (BEM) simulations involving the monopole as a noise source are often used to feed the model creation. However, such a simple source has been demonstrated not to be able to satisfactory model the jet noise [18]. In some low-order models, the noise sources of a single circular jet were represented by a set of uncorrelated quadrupoles [19]. However, it was shown that the directivity at shallow angles was not well reproduced [20].

In this framework, the discovery of coherent structures in jets changed the perspective of jet noise and provided a basis for introducing the wave–packet approach [21]. As suggested by Papamoschou [22], the wave–packet is an amplitude-modulated travelling pressure wave. Several authors have widely used this approach to predict and model the jet noise source from far-field measurements having parameters such as envelope amplitude, wavelength, position, and convection velocity (see e.g. references [23, 24]). For example, Cavalieri et al. [25] used azimuthally decomposed far-field measurements to determine envelope parameters for higher-order azimuthal modes. However, for the mentioned BWB architecture, the jet is typically in a very closely coupled configuration with the center body scattering surface. A large body of literature demonstrated that the low-frequency amplification of the jet noise in the classical jet-wing architecture can be ascribed to the scattering of the jet hydrodynamic field [26–28]. The prediction of the acoustic shielding, hence, needs source models able to capture the near field characteristics of the emitted noise in order to accurately address the effects of the aircraft scattering. Applications of the wave–packet procedure using near-field measurements have been carried out in various research works. Mollo-Christensen [29, 30] provided the first observations of the wave–packet features from the point of view of hydrodynamic instability and aeroacoustics, whereas Crighton and Huerre [31] suggested various simple models to predict near-field structures. Following the literature, the near-acoustic field is characterized by acoustic fluctuations that are small enough to permit linearization but close to the jet so that they could be contaminated by the irrotational hydrodynamic pressure field. In this region, most of the kinetic energy of fluctuations is related to azimuthally-coherent structures that lead to nonlinear effects on the wave–packet evolution. Thus, for the complexity mentioned above, the high subsonic jet noise source prediction is still a challenging

task, which is crucial because it represents the operative condition of modern turbofan engines. In this framework, the principal focus of the present work is to find out an optimized amplitude-modulated wave–packet able to model the jet near-field noise that can be integrated in future into the BEM formulation to obtain a reliable prediction of the jet-surface aeroacoustic scattering also for innovative aircraft configurations. To tune the present model, we used a numerical database obtained using a LES simulation of an isothermal round free jet at a Mach number of $M = 0.9$ and a diameter-based Reynolds number of $Re_D = 10^5$ with the nozzle exhaust turbulence level fixed at $TI = 9\%$. The database contains pressure data at different axial and radial locations, that we considered in a subset ranging from x/D=0 up to x/D=20 in the axial direction and from $r/D = 0.5$ up to $r/D = 3$ in the radial direction, allowing us to optimize the wave–packet jet near-field domain. The near-field domain depicted in this database is representative of all the jet zones that could be influenced by solid boundaries in reality (*i.e.* wing or fuselage) see, [26, 27].

A preliminary version of this study has been presented at the 28th AIAA/CEAS Aeroacoustics 2022 Conference [32], in which the optimization of the wavepacket involved a single Strouhal number. This paper reports an extensive analysis performed at multiple Strouhal numbers, namely $St_D = fD/U_j = 0.25$, 0.5, 0.75 and 1 where f and U_j are the frequency and the nozzle exhaust jet velocity respectively, and for the 0^{th} azimuthal mode which has a relevant intermittency around the frequencies associated with the lower Strouhal numbers [33, 34]. This has been confirmed by Cavalieri [25], who found a superdirective wavepacket to be consistent with the polar structure of the sound field for azimuthal Fourier modes $m = 0$, 1 and 2 and $0.2 < St_D < 0.8$ [35]. As suggested by Rodriguez et al. [36], at low and moderate Strouhal numbers, the 0^{th} mode is the most relevant one for the noise radiated by single jets. This is due to the more elongated structure of the corresponding wave–packet, the higher peak amplitudes, and slower radial decay. For this reason, this mode can be considered representative of the whole signal in the analyzed domain, and being this the first work that considers near–field data in the optimization of the wavepacket, we take into account only the axisymmetric mode $m = 0$. The optimization has been performed using a Multi-Objective Particle Swarm Optimization (PSO) algorithm [37], originally introduced by Kennedy and Eberhart [38], which is based on the social–behavior metaphor of a flock of birds or a swarm of bees searching for food, and belongs to the class of heuristic algorithms for evolutionary derivative-free global optimization.

The paper is structured as follows. Key information about the numerical simulation used to generate the database are presented in section II. In section III details about the wave–packet model are reported and the optimization algorithm. Results are shown in section IV. Some concluding remarks are proposed in section V.

II. Numerical setup

The near-field of the isothermal round free jet at a Reynolds number $Re_D = 10^5$ used for this paper has been computed by (LES). The nozzle exhaust jet Mach number has been fixed at $M = 0.9$, with the nozzle-exhaust boundary-layer thickness set at $\delta_{bl} = 0.15r_0$ and the nozzle exit turbulence intensity at 9% (see [39] for details). The LES has been

carried out using an in-house solver of the three-dimensional filtered compressible Navier-Stokes equations in cylindrical coordinates (r, θ, x) based on low-dissipation and low-dispersion explicit schemes. The quality of the grid for the present jet LES has been assessed in previous papers [40]. Specifically, the grid contains approximately one billion points. Pressure has been recorded at several locations spanning a large near-field domain and gaining time-resolved signals, see references [40], and [41] for a description of the available data. In addition, the near-pressure field of this jet has been also investigated in [42]. Being the present study limited to the near-field domain, we consider arrays of virtual microphones parallel to the nozzle exhaust, positioned at r/D=1, 2, 2.5, and 3. Each array contains 1024 probes that cover a domain that spans between x=0 up to x/D=20. The data have been stored at a sampling frequency corresponding to St_D = 12.8, with a total of 3221 time snapshots. A representative one is shown in Fig.1. The LES dataset selected for the present work is over-resolved for the purpose, and less resolved simulations or, also, experimental data might be, in principle, used successfully. Nevertheless, we preferred a very well-assessed simulation with a very high spatial resolution for this first study on optimizing a wavepacket with near-field data. The original pressure signals are represented in terms of their azimuthal components through the azimuthal decomposition [43]. The Fourier coefficients are stored for the first four azimuthal modes that dominate the sound field for low polar angles. As aforementioned the wavepacket model presented in this paper has been carried out for the 0^{th} azimuthal mode, which is dominant for the noise generation at Strouhal numbers lower than 1 [25].

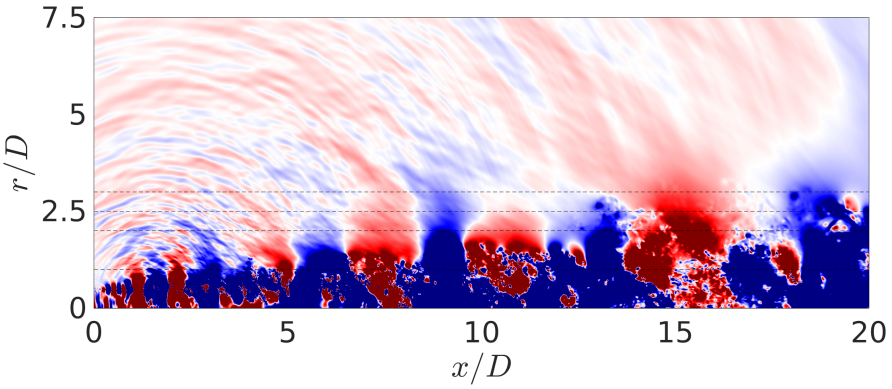

Fig. 1 Snapshot in the (x,r) plane of the pressure signals. The black dashed lines represent the probe arrays.

III. Wave–packet model

The noise source model used, *i.e.* the wave–packet model for the jet noise, has been introduced by Papamoschou in references [18, 22, 23, 44], who in turn developed it from the works by Morris [45, 46] and the previous ones by Tam and Burton [47], Crighton and Huerre [31], and Avital *et al.* [48]. The fundamental assumption at the basis of the model is that the peak noise radiation from the jet in the aft region is related to the large-scale coherent structures in the jet flow which can be modeled as instability waves at its boundary, growing and then decaying along the axial distance

[18]. In the model, the jet is substituted with a cylindrical surface, surrounding the original jet, radiating the pressure perturbation imposed on it. Applying the wave–packet ansatz, the pressure on the cylindrical surface at r_0 surrounding the jet is prescribed as

$$p_w(m, r_0, x, \theta, t) = p_0(x) e^{-i\omega t + im\theta} \tag{1}$$

where m is the azimuthal mode number, x denotes the axial coordinate, θ is the azimuthal angle, $\omega = 2\pi f$ is the pulsation. In the present study, the reference surface is taken at $r_0 = D$ and the wave–packet axial shape $p_0(x)$ is given in the form [18]

$$p_0(x) = \tanh\left(\frac{(x - x_0)^{p_1}}{b_1^{p_1}}\right)\left[1 - \tanh\left(\frac{(x - x_0)^{p_2}}{b_2^{p_2}}\right)\right] e^{i\alpha(x - x_0)} \tag{2}$$

The coordinate x_0 is used to locate the relative position between the origin of the wave–packet function and the nozzle exit. The signal growth is controlled by the parameters b_1 and p_1, while b_2 and p_2 define its decaying rate. Following Morris [46] and Papamoschou [18], the solution in the linear regime (*i.e.*, solution for the 3D wave equation in cylindrical polar coordinates) for an arbitrary radial distance $r \geq r_0$ can be evaluated as

$$\begin{aligned} p_w(m, r, x, \theta, t) &= \frac{1}{2\pi} e^{-i\omega t + im\phi} \int_{-\infty}^{\infty} \hat{p}_0(k) \frac{H_m^{(1)}(\lambda r)}{H_m^{(1)}(\lambda r_0)} e^{ikx} dk \\ \text{with} \quad \lambda &= \left[\left(\frac{\omega}{c_\infty}\right)^2 - k^2\right]^{1/2}, \qquad -\frac{\pi}{2} < arg(\lambda) < \frac{\pi}{2} \end{aligned} \tag{3}$$

where $\hat{p}_0(k)$ is the Fourier transform of $p_0(x)$, c_∞ is the speed of sound of the unperturbed flow, and $H_m^{(1)}$ is the Hankel function of the first kind and order m. The model adopted is derived from the 3D wave equation in cylindrical coordinates, which solution is radially decaying as a combination of a Bessel of the first and second kind (*i.e.* a Hankel function of the first kind [46]). The pressure field generated by the wave–packet can be easily separated in its radiative and decaying components looking at the supersonic ($|\omega/k| \geq c_\infty$) and subsonic ($|\omega/k| < c_\infty$) values of the phase speed, respectively.

In Papamoschou [18], the parameters of the deterministic wave–packet were obtained through a numerical optimization aimed at matching the experimentally measured far field directivity of the jet, hence involving only the radiative part of the wave–packet. The tuned wave–packet was then employed as an equivalent noise source for the jet in BEM scattering calculations to predict the shielding effect from a thin plate. However, the interactions between the pressure perturbation generated by the wave–packet and the obstacle typically happen in the jet near-field. The wave–packet axial location was adjusted to match the near-field peak emission obtained from phased-array measurements to include some information on the acoustic near-field.

In this work, the same deterministic wave–packet model is used, but its parameters are defined from near-field data on co-axial lines at several radial distances from the jet axis, namely $r/D = 1$, 2, and 2.5. A multi-objective

optimization procedure aims at matching the complete pressure fluctuation envelope from the model with the one from the numerical simulations for each of the considered lines. A generic unconstrained optimization problem consists of the research of the set of variables $\mathbf{v}$ that yields to a minimum of the N_J objective functions $J_n(\mathbf{v}, \mathbf{q})$

$$\begin{aligned} &\text{minimize/maximize } [J_n(\mathbf{v}, \mathbf{q})], \qquad n = 1, ..., N_J \text{ and } \mathbf{v} \in \mathcal{D}_\mathbf{v} \\ &\text{with bounds } v_m^L \leq v_m \leq v_m^U, \qquad m = 1, ..., N_v \end{aligned} \tag{4}$$

where $\mathbf{q}$ is the vector of the parameters, $\mathbf{v}$ is the vector of the N_v design variables bounded by v_n^L and v_n^U in the design space $\mathcal{D}_\mathbf{v}$, In the present application, $\mathbf{v}$ represents the vector collecting the wave–packet parameters $\mathbf{v} = \left[p_1, b_1, p_2, b_2, \omega/(\alpha U_j), x_0\right]$ and $N_J = 3$ defines the three objective functions to be minimized, one for each r_n considered

$$J_n(\mathbf{x}, \mathbf{y}) = \sqrt{\int \left(\frac{|p_n(r_n) - p_{LES}(r_n)|}{\max\left(|p_{LES}(r_n)|\right)} \right)^2 dx} \tag{5}$$

The objective functions represent the L2-norm of the difference between the pressure predicted by the wavepacket source model and the reference pressure from the LES over the axial extension of the considered lines, divided by the peak value from the reference curve for each radial distance to normalize the objective function values. Multiple Strouhal numbers have been considered, optimizing the wavepacket source model separately for each value in the set $St_D = 0.25,\ 0.5,\ 0.75$ and 1, using pressure data from the numerical database for the dominant axisymmetric azimuthal mode. With the values of the three objective functions tending to zero simultaneously, the wave–packet model would perfectly trace the simulations for the considered radial distances. A solution reaching this goal would occupy the so-called utopia point in the codomain, which, as its name suggests, is not reachable for non-trivial multi-objectives problems in which the involved functions are even just partially conflicting. In these cases, including the one considered in this paper, the optimization process identifies a set of compromise solutions that identify an (approximated) Pareto front in the codomain. The defining property of solutions lying on a Pareto frontier is that moving from one to the other none of the objective functions can be improved in value without degrading some of the other. Hence, the Pareto front identifies all the, possibly infinite, non-dominated solutions of the multi-objective optimization problem, which is considered optimal in a Paretian sense, and equally good. Any choice of the preferred solution within this set is subjective, and to be made depending on the problem under analysis with a specific grade of arbitrariness [49, 50].

IV. Results

Since the interest is primarily on matching the shape of the modelled pressure at several radial distances and the relative amplitudes among them rather than the absolute ones, the data from the simulations have been normalized with respect to the maximum value at r_0. For each St_D, a Multi-Objective Particle Swarm Optimization algorithm is employed to find the solutions minimizing all the objective functions together. This heuristic optimization algorithm

introduced originally by Kennedy and Eberhart [38] was extended to handle multiple objective functions by Coello *et. al.* [37, 51]. The optimization has been performed with a Matlab implementation using a fixed budget of 500 iterations, with a swarm composed of 140 individuals, whose initial positions were randomly defined in the domain with uniform distribution~~,for a total time of about 200s per optimization on a single core~~. . The total computation time on a workstation with an Intel Xeon(R) CPU E5-2620 v4 @ 2.10GHz took about 200s per optimization on a single core. The subroutines might be better optimized to further reduce the computation time. At the present moment, the method is applicable to one azimuthal mode at a time, and when more than one is expected to give a significant contribution, the total noise source can be obtained with a linear combination. A possible future extension of the method might simultaneously optimise more than one wavepacket, each one with a different azimuthal mode. The drawback of this approach is that a good solution is expected to be more difficult to be found as the dimension of the domain increases (there will be four variables per wavepacket); this problem is typically referred to as "the course of dimensionality".

As anticipated in the previous section, when the objectives conflict, the solutions resulting from the minimization are optimal in a Paretian sense. The set of Pareto-optimal solutions lying on the Pareto front plotted in Fig.2, has equal dignity in terms of minimization of the objective functions. Since it represents the set of the non-dominated solutions, moving along the front is not possible to improve one of the objective values without worsening at least one of the others. One of the techniques that may be employed to identify the preferred solution among the optima is to identify a ranking criterion [15, 49, 52–54] (also called Decision Maker algorithm), to be used as an added objective, evaluating the solutions performance on it and then selecting the solution resulting in the most suitable. Any selection criterion is valid in principle and may be used reasonably, from simple subjective preferences to more complex analyses of the results. In this study, a Pareto ranking criterion is formulated by combining the analysis of the performance of the optimized source model when predicting the pressure fluctuations over the $n+1$ line at $r_{n+1}/D = 3$ (a farther radial distance from the ones used during the optimization), and the distance of the solutions from the utopia point in the codomain of the problem. In particular, solutions are ordered on the basis of their J_{n+1} value, and all the solutions with a relative difference in their value under 100% with respect to the best one are included in a subset of optimal solutions; the one closest to the utopia point is taken as the preferred one. The only exception is the $St_D = 0.5$ case, in which the solution minimizing the error on the closest line $r/D = 1$ is selected. This kind of decision-maker (DM) algorithm can be classified in the class of the *a posteriori articulation of preferences* [52], implying that the DM's involvement starts posterior to the explicit revelation of "interesting" solutions.

In Fig.2 the optimal solutions are highlighted by red circles on their respective three dimensional Pareto fronts. Each dot representing a solution is coloured on the basis of its fitness over the $n+1$ line. It can be seen that the Pareto ranking criterion tends to prefer solutions that privilege the results on J_1 and J_3 more than the performance on the second radial distance J_2.

Figure 3 shows the shapes of the optimal wave–packets identified by the Pareto ranking criterion. The envelope

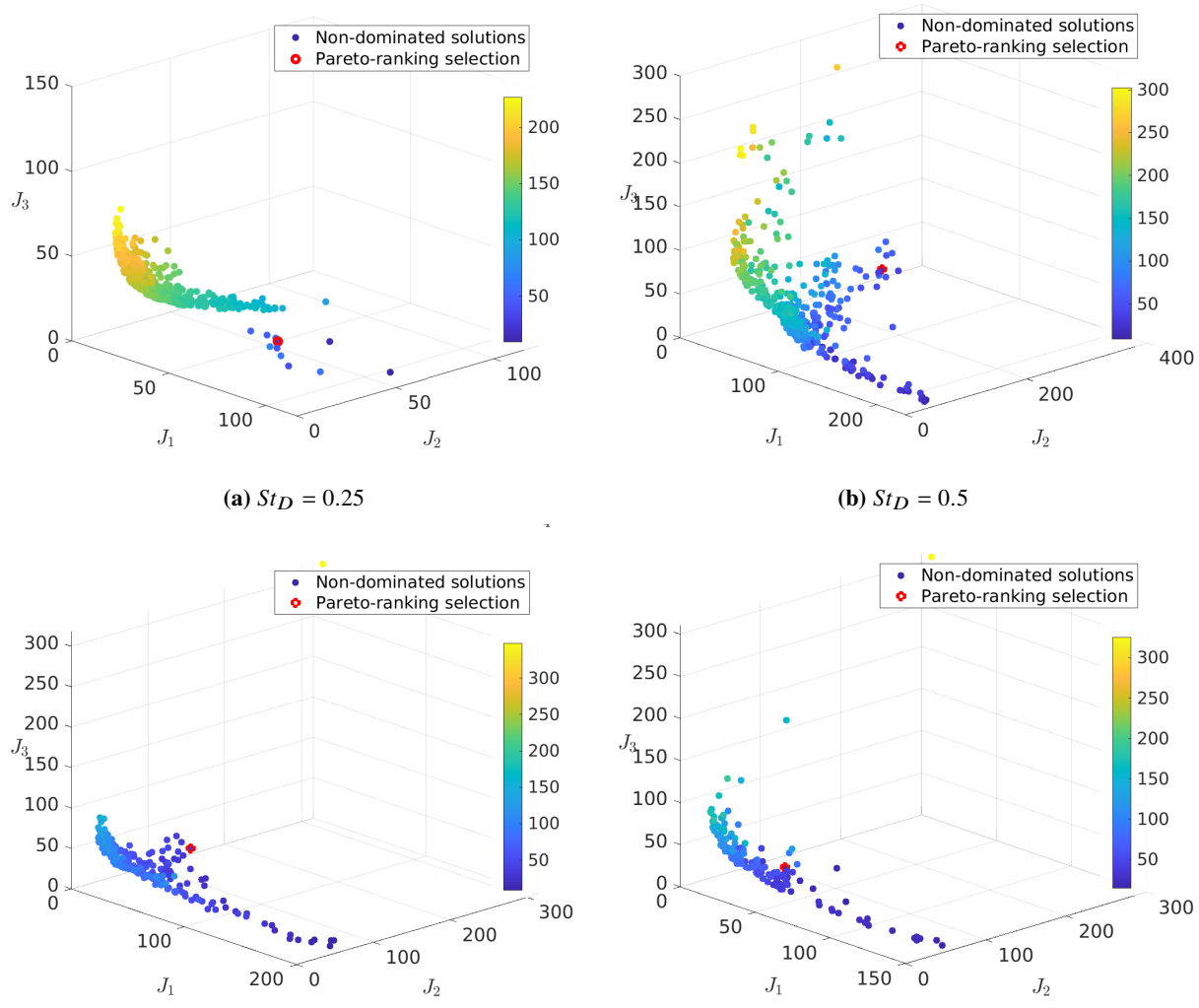

(a) $St_D = 0.25$ **(b)** $St_D = 0.5$

(c) $St_D = 0.75$ **(d)** $St_D = 1.0$

Fig. 2 Codomains of the optimization problems. Non-dominated solutions of the multi-objective optimization for the analysed Strouhal numbers.

of the complex pressure is represented in black, with the real and imaginary parts plotted with blue and red lines, respectively. The sound emission of a wave–packet source depends on both the spatial envelope and temporal growth and decay [31, 55]. As expected, the wave–packet shapes strongly depend on the Strouhal number, which affects in particular the peak amplitude location. It can be seen that the number of spatial oscillations inside the envelope increase with the Strouhal number, as the spatial and temporal frequencies are linearly connected by the sound speed.

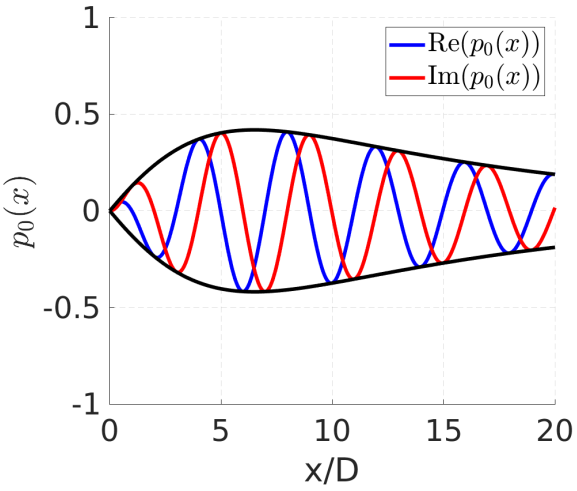

(a) $St_D = 0.25$ -
$\mathbf{v_{opt}} = [1.0558, 6.03, 0.7017, 16.8122, 1.0112, 0.0001]$

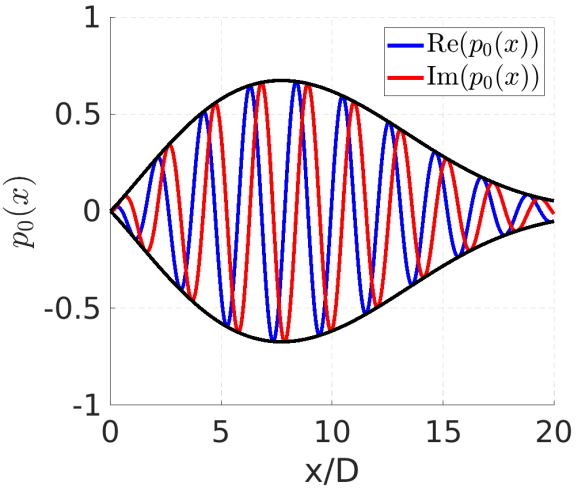

(b) $St_D = 0.5$ -
$\mathbf{v_{opt}} = [1.0664, 6.8254, 2.4476, 15.7218, 1.0625, 0.0018]$

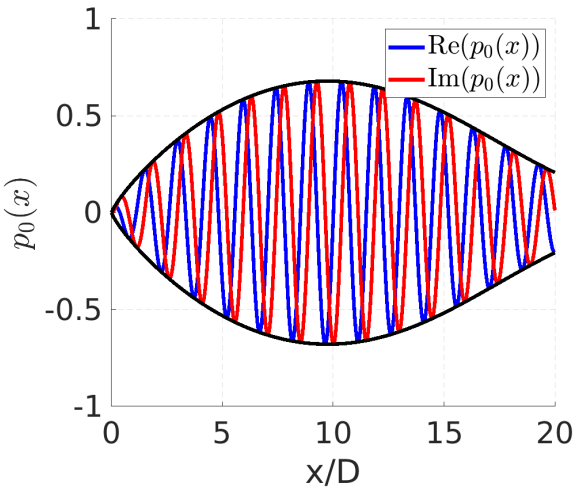

(c) $St_D = 0.75$ -
$\mathbf{v_{opt}} = [0.8120, 9.2314, 2.9113, 19.6413, 1.1268, 0.0122]$

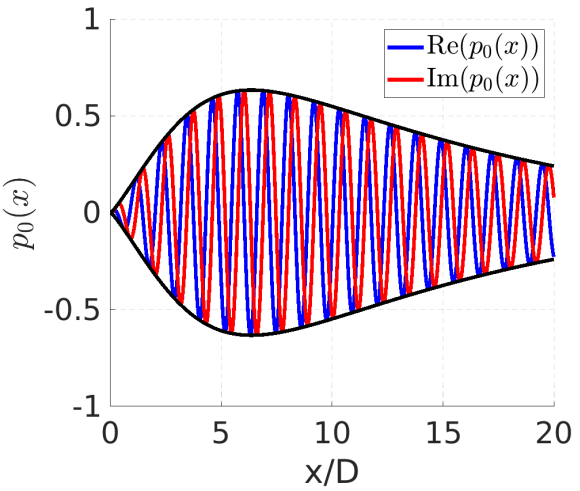

(d) $St_D = 1.0$ -
$\mathbf{v_{opt}} = [1.1596, 4.7583, 1.0663, 20.0931, 1.1350, 0.0169]$

Fig. 3 Shape of the optimized wave–packets and their parameters.

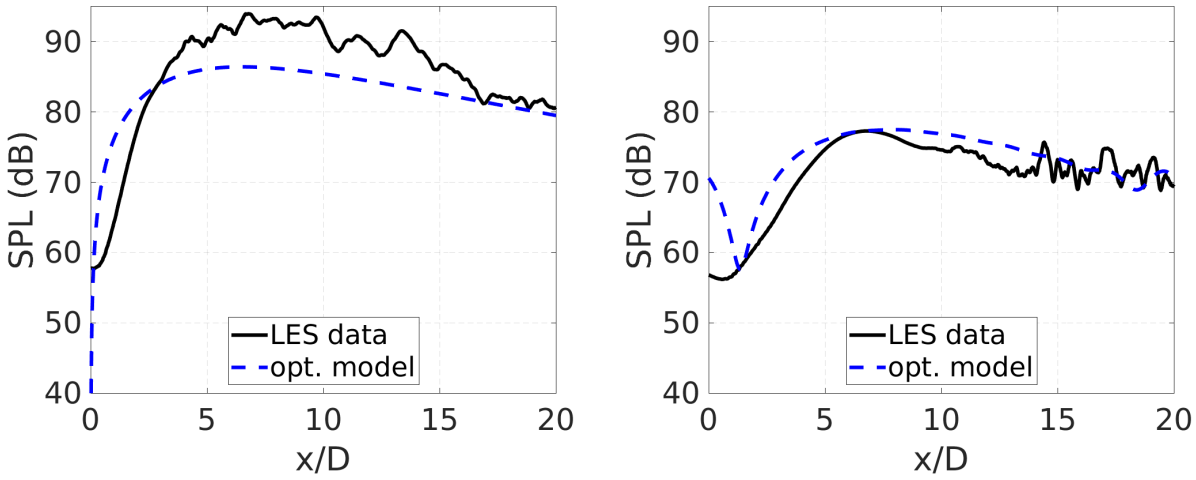

(a) r/D = 1

(b) r/D = 2

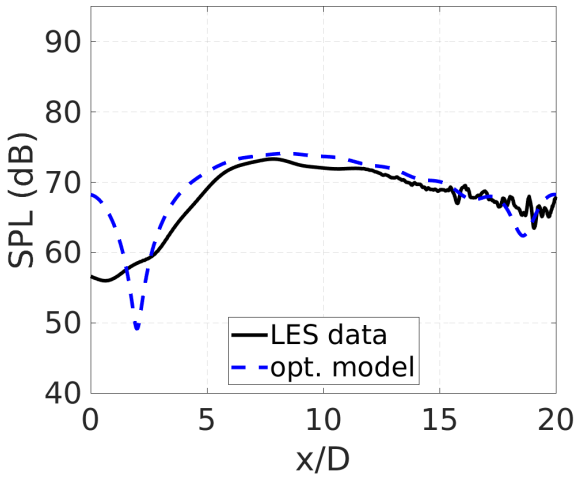

(c) r/D = 2.5

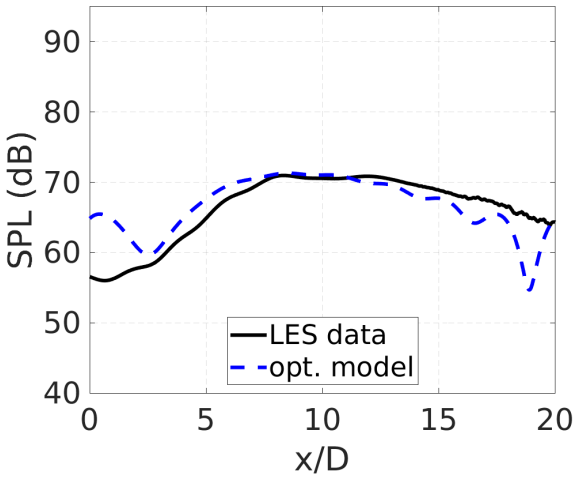

(d) r/D = 3

Fig. 4 Solution selected by the Pareto ranking criterion for $St_D = 0.25$. Results for the radial distances used in the optimization (a)-(c) and for the validation line (d).

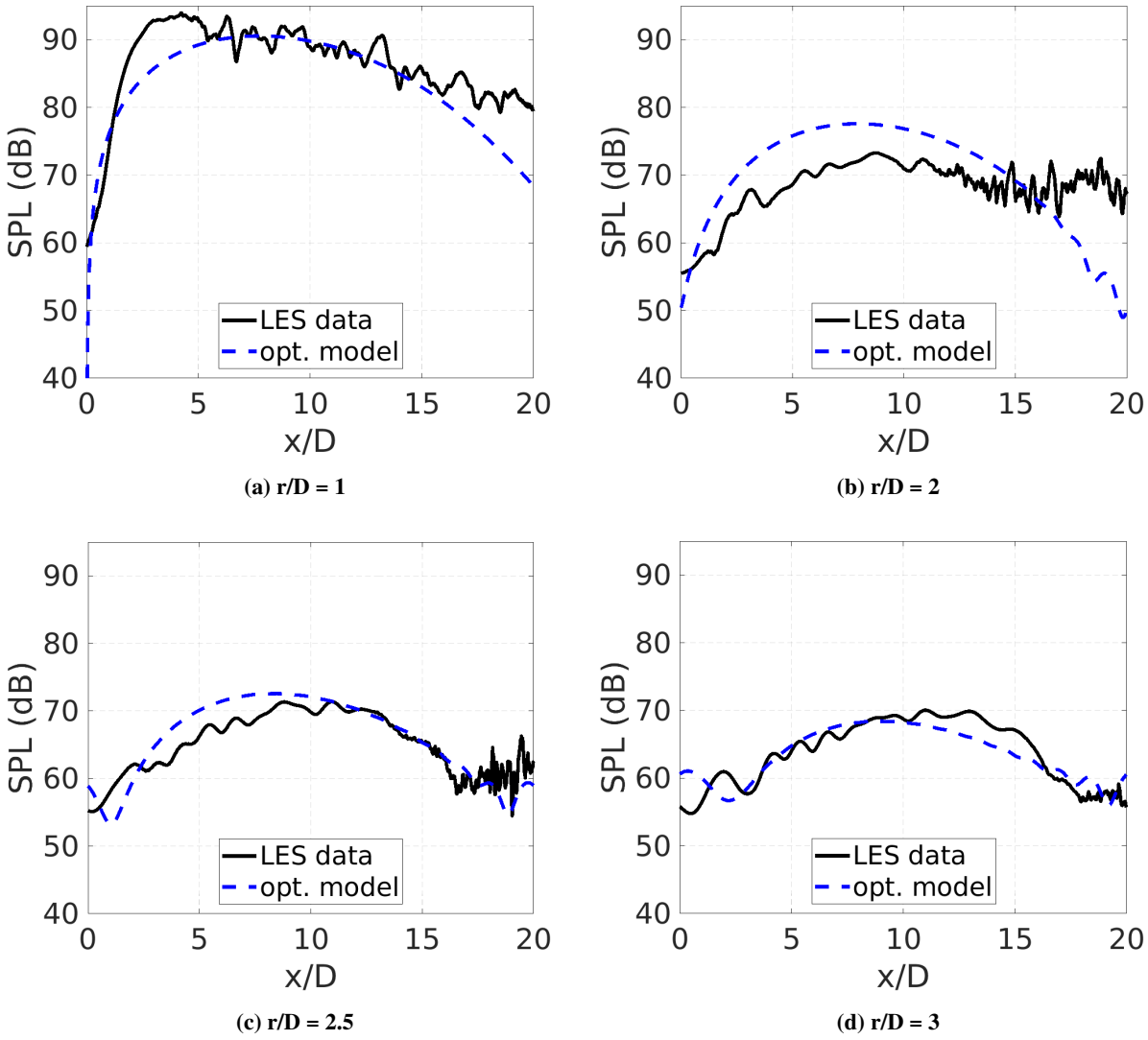

(a) r/D = 1 **(b) r/D = 2**

(c) r/D = 2.5 **(d) r/D = 3**

Fig. 5 Solution selected by the Pareto ranking criterion for St_D = 0.5. Results for the radial distances used in the optimization (a)-(c) and for the validation line (d).

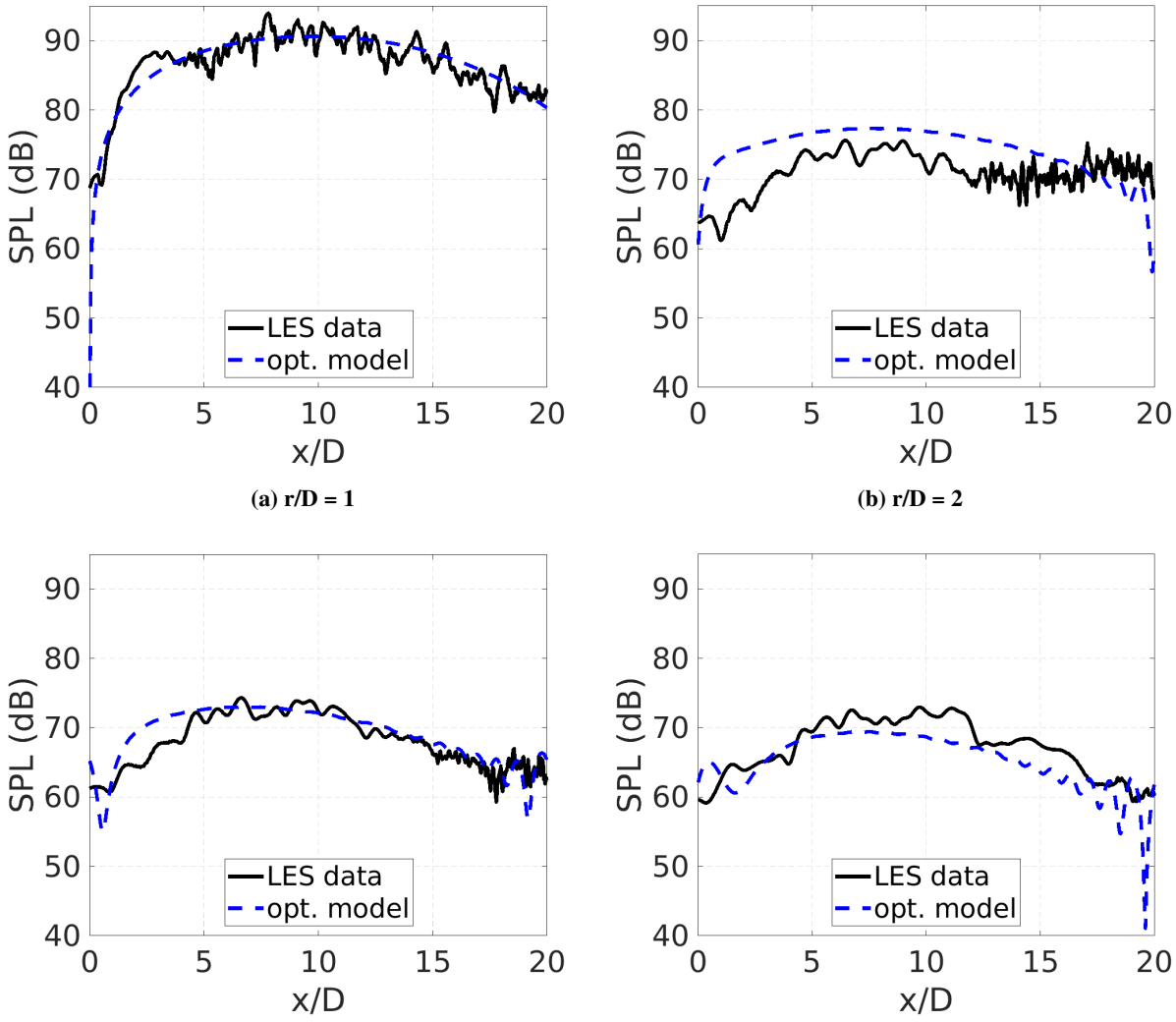

(a) r/D = 1 **(b) r/D = 2**

(c) r/D = 2.5 **(d) r/D = 3**

Fig. 6 Solution selected by the Pareto ranking criterion for $St_D = 0.75$. Results for the radial distances used in the optimization (a)-(c) and for the validation line (d).

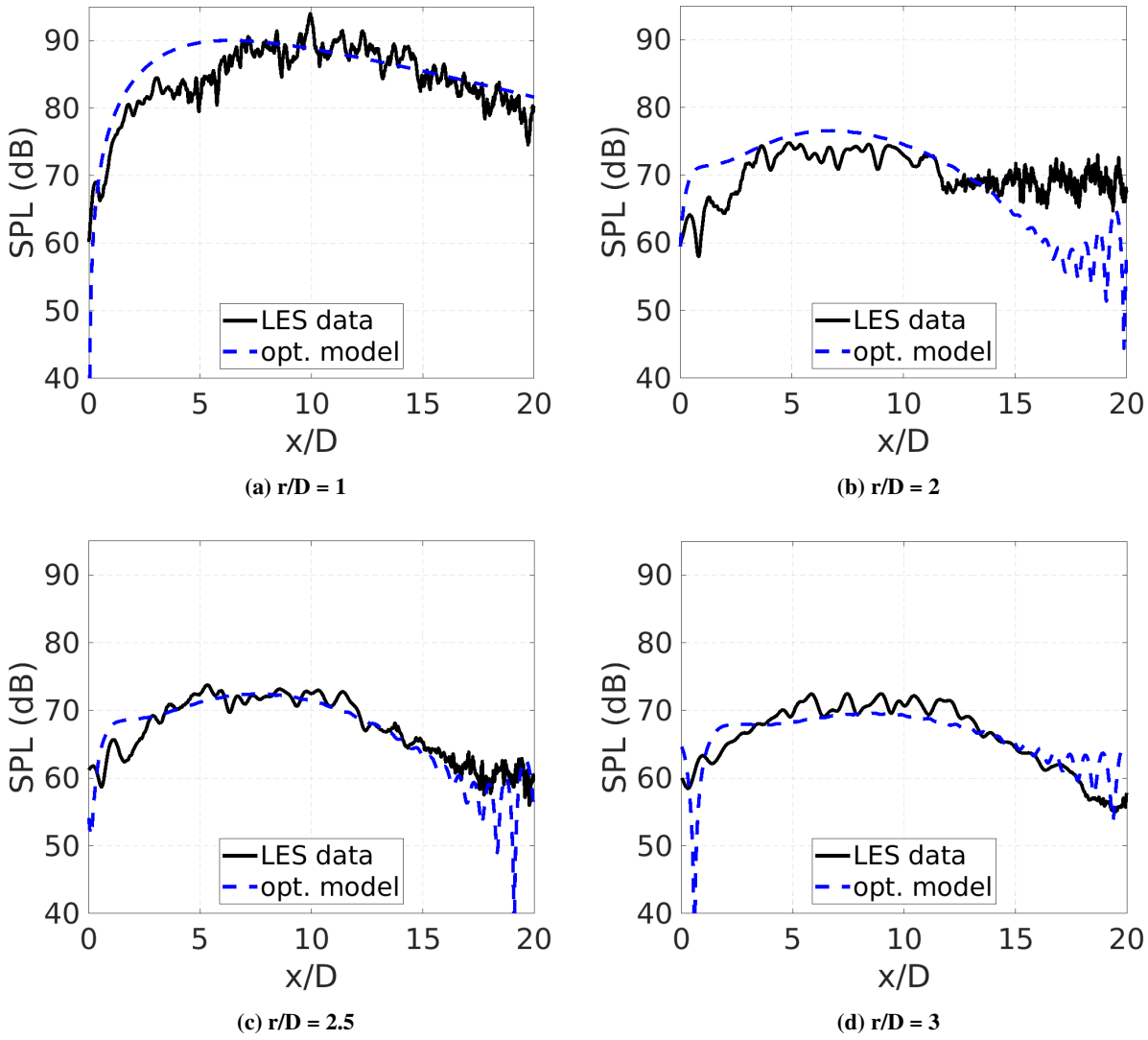

Fig. 7 Solution selected by the Pareto ranking criterion for $St_D = 1$. Results for the radial distances used in the optimization (a)-(c) and for the validation line (d).

Figures 4–7 shows the sound pressure levels (SPL) predicted by the LES simulations and by the optimised wave–packets at the four St_D and radial distances considered. The optimized wave–packets selected with the Pareto ranking criterion give satisfactory agreement with the LES SPL on the lines located at r/D =1, 2 and 2.5 used in the optimization for all the Strouhal analysed in Figures 4–7 (a–c). A good prediction of the pressure perturbation by the wave–packet model is also observed at $r/D = 3$ in Figures 4–7 (d). It should be noted that the propagation of the pressure perturbation considered by the wave–packet model assumes that the radiating surface is outside of the jet plume, while the first line at $r/D = 1$ is immersed in the flow for large part of its axial extension. It is necessary to use this kind of approximation of the model to include the near–field hydrodynamic contribution inside the optimized source, which is important to predict the scattering noise generated by a jet installed close to a solid boundary. Without

a good match on the propagated information at $r/D = 3$, the wave–packet prediction capabilities would be comparable to an interpolation model. On the contrary, the agreement on the fourth line confirms that the optimized wave–packets correctly catch some of the jet noise source characteristics and the relative importance of the hydrodynamic and acoustic part of the pressure perturbation, since the wave–packets were not informed of the LES pressure fields for r/D>2.5.

St_D	r/D = 1	r/D=2	r/D=2.5	r/D=3
0.25	4.9	2.4	2.1	2.4
0.5	3.6	5.8	2.2	1.8
0.75	1.7	4.2	1.6	2.6
1.0	3.0	4.6	1.9	2.1

Table 1 Mean error in dB on each virtual probe line between predicted and LES levels for each Strouhal number.

The mean difference between the wave–packet and the LES SPL curves is representative of the model's average error. The values for all radial distances and Strouhal numbers are reported in Tab. 1. They are lower than 3 dB for 75% of the analysed data. Some grade of conflict of the objective functions is somehow expected. The ideal jet noise source model would simultaneously fit the reference pressure curves at all distances, leading to a unique optimum solution instead of a Pareto front. However, it has to be reminded that the wave–packet model used in this study is a simplified interpretation of the actual noise production and propagation phenomena related to the jet. The line at $r/D = 1$, moreover, is partially immersed in the jet, due to the jet expansion angle, while the wave–packet model assumes the pressure propagation to higher radial distances to happen in a quiescent fluid. The use of the information on this line introduces an approximation in the model, which, however, needs to be informed with perturbations from the very proximity of the jet axis to predict also the hydrodynamic field.

V. Conclusion

For the first time, a multi–objective optimization of a wave–packet in the jet near–field is presented to predict the behaviour of the 0^{th} azimuthal mode. The results of the optimizations are found to provide a good agreement between the numerical reference data and the model in the tested Strouhal range $0.25 \leq St_D \leq 1$. The optimizations have been performed for a wide range of Strouhal numbers where the 0^{th} mode is known to be an essential component in the whole jet pressure field, and for radial distances relevant for the jet-surface scattering phenomena in innovative aircraft configurations.

A Pareto front has been obtained as a solution of each optimization due to the objectives being partially conflicting, *i.e.* the model-simulation agreement at three different radial distances from the jet axis. The preferred solution on the front is then selected using a Pareto ranking criterion method, considering the wavepacket prediction over an extra line. The optimized noise source model prediction can reproduce the LES data from the free jet with a mean error for each

radial distance of the probe arrays within 3 dB for most cases and is suitable to be integrated into the BEM solver to evaluate of jet-surface aeroacoustic scattering. Specifically, the idea, which is currently under development, is to use this optimized noise source to generate the incident field over the scattering body (such as the wing pressure side for standard aircraft, or the trailing part of a BWB center body section), and then evaluate solution for the jet installed noise including the scattering and shielding effects from the surfaces. In the presented approach, being the wavepacket related to a free jet, in order to address different engine-airframe arrangements it is sufficient to adjust the evaluation of the incident field, changing only the relative positioning between the noise source and the scattering surfaces without modifying the wavepacket parameters. The process can be easily included in an optimization loop to find the solution minimizing, for example, the noise radiated towards the ground. The computational related to the acoustic simulation of each configuration can be significant, in particular for high frequency acoustic simulations, making the whole optimization process barely or even not affordable. To mitigate the effort required, some metamodeling techniques can be applied. Among other techniques, adaptive radial basis functions (also in their stochastic version) and/or artificial neural networks may be used, which have been recently applied to the metamodelling of similar problems, both for shielding and jet noise prediction [16, 17]. Such surrogate models allow for very fast evaluations of the specific metrics they are built for, *e.g.* insertion loss at some observation points, dramatically reducing the optimization cost. The computational effort is substantially moved to the building of the metamodel, which must be trained with some (possibly costly) acoustic simulations, however it is expected to be lower than what a direct approach would require.

The optimized wave–packet capability to predict the solution at a higher radial distance shows that it captures at least some of the features of the modelled noise source, such as the relative contributions of the radiating and non radiating parts of the pressure perturbations. It has been evidenced how the probe line closer to the jet axis is partially immersed in the flow, which is somehow a limit of the model. However, the final aim of the work is to develop a jet noise source model able to predict the scattering effects in closely coupled installed jet configurations, where the flow grazes the scattering surfaces and the hydrodynamic part of the perturbation is relevant. The method is, in principle, applicable to any noise signal produced by jets in which the contribution from coherent structures is significant. Furthermore, the input for the wavepacket optimization is not restricted to numerical simulations, as experiment data is also eligible. In any case, if we consider turbulent jets and the underlying hypotheses of the wavepacket modelling of jet noise are satisfied, the optimization procedure is expected to be able to find a set of parameters for the wavepacket, also for a Reynolds number typical of flight conditions (i.e. about two orders of magnitudes higher of what has been considered in this study). The method can also be coupled with existing empirical scaling law to estimate the SPL for different flow conditions, including Mach number variations[56, 57] and partially considering the effect of the Reynolds number [57, 58]. It is worth noting that two orders of magnitude of Reynolds number can involve a variation of the shape of the SPL spectrum, yielding in non-perfect effectiveness of the empirical laws at all the St numbers. Further investigations that involve multimodal analyses including other azimuthal contributions and different turbulence levels are ongoing.

The multimodal approach will be needed to extend the presented model towards complex geometries, like ~~C~~hevrons and ~~S~~carfed nozzle, in which jet flows are no longer characterized by axial symmetry, and hence higher azimuthal order modes need to be involved in the analysis.

Acknowledgments

C. Bogey was partially supported by the LABEX CeLyA (ANR-10-LABX-0060/ANR-16-IDEX-0005). The numerical data analyzed in this work were obtained using the HPC resources of PMCS2I (Pôle de Modélisation et de Calcul en Sciences de l'Ingénieur et de l'Information) of Ecole Centrale de Lyon, and the resources of IDRIS (Institut du Développement et des Ressources en Informatique Scientifique) under the allocation 2021-2a0204 made by GENCI (Grand Equipement National de Calcul Intensif).

References

[1] Burghignoli, L., Di Marco, A., Centracchio, F., Camussi, R., Ahlefeldt, T., Henning, A., Adden, S., and Di Giulio, M., "Evaluation of the noise impact of flap-tip fences installed on laminar wings," *CEAS Aeronautical Journal*, Vol. 11, No. 4, 2020, pp. 849–872. https://doi.org/10.1007/s13272-020-00454-x.

[2] Kamliya Jawahar, H., Meloni, S., Camussi, R., and Azarpeyvand, M., "Experimental Investigation on the Jet Noise Sources for Chevron Nozzles in Under-expanded Condition," *AIAA Aviation 2021 Forum*, 2021, p. 2181.

[3] Meloni, S., and Kamliya Jawahar, H., "A Wavelet-Based Time-Frequency Analysis on the Supersonic Jet Noise Features with Chevrons," *Fluids*, Vol. 7, No. 3, 2022, p. 108.

[4] Palma, G., and Burghignoli, L., "On the integration of acoustic phase-gradient metasurfaces in aeronautics," *International Journal of Aeroacoustics*, Vol. 19, No. 6-8, 2020, pp. 294–309. https://doi.org/10.1177/1475472x20954404.

[5] Palma, G., Burghignoli, L., Centracchio, F., and Iemma, U., "Innovative Acoustic Treatments of Nacelle Intakes Based on Optimised Metamaterials," *Aerospace*, Vol. 8, No. 10, 2021. https://doi.org/10.3390/aerospace8100296.

[6] Jones, M. G., Nark, D. M., and Schiller, N. H., *Evaluation of Variable-Depth Liners with Slotted Cores*, 2022. https://doi.org/10.2514/6.2022-2823.

[7] Dodge, C., Howerton, B. M., and Jones, M. G., *An Acoustic Liner with a Multilayered Active Facesheet*, 2022. https://doi.org/10.2514/6.2022-2902.

[8] Palani, S., Murray, P., McAlpine, A., Knepper, K., and Richter, C., *Experimental and numerical assessment of novel acoustic liners for aero-engine applications*, 2022. https://doi.org/10.2514/6.2022-2900.

[9] Liebeck, R. H., "Design of the Blended Wing Body Subsonic Transport," *Journal of Aircraft*, Vol. 41, No. 1, 2004, pp. 10–25. https://doi.org/10.2514/1.9084.

[10] Centracchio, F., Burghignoli, L., Rossetti, M., and Iemma, U., "Noise shielding models for the conceptual design of unconventional aircraft," *INTER-NOISE 2018 - 47th International Congress and Exposition on Noise Control Engineering: Impact of Noise Control Engineering*, 2018.

[11] Burghignoli, L., Centracchio, F., Iemma, U., and Rossetti, M., "Multi-objective optimization of BWB aircraft for noise shielding improvement," *25th International Congress on Sound and Vibration 2018, ICSV 2018: Hiroshima Calling*, Vol. 2, 2018, p. 1256 – 1263.

[12] Xie, J., Cai, Y., Chen, M., and Mavris, D. N., *Integrated Sizing and Optimization of Hybrid Wing Body Aircraft in Conceptual Design*, 2019. https://doi.org/10.2514/6.2019-2885.

[13] Papamoschou, D., and Mayoral, S., "Jet noise shielding for advanced hybrid wing-body configuration," *49th AIAA Aerospace Sciences Meeting including the New Horizons Forum and Aerospace Exposition*, 2011, p. 912.

[14] Denisov, S., and Korolkov, A., "Investigation of noise-shielding efficiency with the method of sequences of maximum length in application to the problems of aviation acoustics," *Acoustical Physics*, Vol. 63, No. 4, 2017, pp. 462–477.

[15] Palma, G., Centracchio, F., and Burghignoli, L., "Optimized metamaterials for enhanced noise shielding of innovative aircraft configurations," *Proceedings of the 27th International Congress on Sound and Vibration, ICSV 2021*, 2021.

[16] Burghignoli, L., Rossetti, M., Centracchio, F., Palma, G., and Iemma, U., "Adaptive RBF with hyperparameter optimisation for aeroacoustic applications," *International Journal of Aeroacoustics*, Vol. 21, No. 1-2, 2022, pp. 22–42. https://doi.org/10.1177/1475472X221079545.

[17] Centracchio, F., Burghignoli, L., Palma, G., Cioffi, I., and Iemma, U., "Noise shielding surrogate models using dynamic artificial neural networks," *INTER-NOISE and NOISE-CON Congress and Conference Proceedings*, Vol. 263, No. 1, 2021, pp. 5216–5224. https://doi.org/10.3397/in-2021-3008.

[18] Papamoschou, D., *Prediction of Jet Noise Shielding*, 2010. https://doi.org/10.2514/6.2010-653.

[19] Kopiev, V. F., and Chernyshev, S. A., "Simulation of azimuthal characteristics of turbulent jet noise by correlation model of quadrupole noise sources," *International Journal of Aeroacoustics*, Vol. 13, No. 1-2, 2014, pp. 39–60.

[20] Denisov, S., Kopiev, V., Ostrikov, N., Faranosov, G., and Chernyshev, S., "Using the Correlation Model of Random Quadrupoles of Sources to Calculate the Efficiency of Turbulent Jet Noise Screening with Geometric Diffraction Theory," *Acoustical Physics*, Vol. 66, No. 5, 2020, pp. 528–541.

[21] Jordan, P., and Colonius, T., "Wave Packets and Turbulent Jet Noise," *Annual Review of Fluid Mechanics*, Vol. 45, No. 1, 2013, pp. 173–195. https://doi.org/10.1146/annurev-fluid-011212-140756.

[22] Papamoschou, D., "Wavepacket modeling of the jet noise source," *International Journal of Aeroacoustics*, Vol. 17, No. 1-2, 2018, pp. 52–69. https://doi.org/10.1177/1475472X17743653.

[23] Papamoschou, D., *Wavepacket Modeling of the Jet Noise Source*, 2011. https://doi.org/10.2514/6.2011-2835.

[24] Kœnig, M., Cavalieri, A. V., Jordan, P., Delville, J., Gervais, Y., and Papamoschou, D., "Farfield filtering and source imaging of subsonic jet noise," *Journal of Sound and Vibration*, Vol. 332, No. 18, 2013, pp. 4067–4088. https://doi.org/https://doi.org/10.2514/6.2010-3779.

[25] Cavalieri, A. V. G., Jordan, P., Colonius, T., and Gervais, Y., "Axisymmetric superdirectivity in subsonic jets," *Journal of Fluid Mechanics*, Vol. 704, 2012, p. 388–420. https://doi.org/10.1017/jfm.2012.247.

[26] Meloni, S., Proença, A. R., Lawrence, J. L., and Camussi, R., "An experimental investigation into model-scale installed jet–pylon–wing noise," *Journal of Fluid Mechanics*, Vol. 929, 2021. https://doi.org/10.1017/jfm.2021.831.

[27] Meloni, S., Mancinelli, M., Camussi, R., and Huber, J., "Wall-pressure fluctuations induced by a compressible jet in installed configuration," *AIAA Journal*, Vol. 58, No. 7, 2020, pp. 2991–3000. https://doi.org/https://doi.org/10.2514/1.J058791.

[28] Jordan, P., Jaunet, V., Towne, A., Cavalieri, A. V. G., Colonius, T., Schmidt, O., and Agarwal, A., "Jet–flap interaction tones," *Journal of Fluid Mechanics*, Vol. 853, 2018, p. 333–358. https://doi.org/10.1017/jfm.2018.566.

[29] Mollo-Christensen, E., "Measurements of near field pressure of subsonic jets," Tech. rep., ADVISORY GROUP FOR AERONAUTICAL RESEARCH AND DEVELOPMENT PARIS (FRANCE), 1963.

[30] Mollo-Christensen, E., "Jet Noise and Shear Flow Instability Seen From an Experimenter's Viewpoint," *Journal of Applied Mechanics*, Vol. 34, No. 1, 1967, pp. 1–7. https://doi.org/10.1115/1.3607624.

[31] Crighton, D. G., and Huerre, P., "Shear-layer pressure fluctuations and superdirective acoustic sources," *Journal of Fluid Mechanics*, Vol. 220, 1990, p. 355–368. https://doi.org/10.1017/S0022112090003299.

[32] Palma, G., Meloni, S., Camussi, R., Iemma, U., and Bogey, C., *A Multi-Objective Optimization of a Wave-Packet Model Using Near-Field Subsonic Jet Data*, 2022. https://doi.org/10.2514/6.2022-2934, URL https://arc.aiaa.org/doi/abs/10.2514/6.2022-2934.

[33] Camussi, R., and Bogey, C., "Intermittent statistics of the 0-mode pressure fluctuations in the near field of Mach 0.9 circular jets at low and high Reynolds numbers," *Theoretical and Computational Fluid Dynamics*, Vol. 35, No. 2, 2021, pp. 229–247. https://doi.org/10.1007/s00162-020-00553-9.

[34] Micci, G. L., Camussi, R., Meloni, S., and Bogey, C., "Intermittency and Stochastic Modeling of Low- and High-Reynolds-Number Compressible Jets," *AIAA Journal*, Vol. 60, No. 3, 2022, pp. 1983–1990. https://doi.org/10.2514/1.J061128.

[35] Albuquerque Maia, I., Jordan, P., Cavalieri, A., and Jaunet, V., "Two-point wavepacket modelling of jet noise," *Proceedings of the Royal Society A: Mathematical, Physical and Engineering Sciences*, Vol. 475, 2019, p. 20190199. https://doi.org/10.1098/rspa.2019.0199.

[36] Rodríguez, D., Jotkar, M. R., and Gennaro, E. M., "Wavepacket models for subsonic twin jets using 3d parabolized stability equations," *Comptes Rendus Mécanique*, Vol. 346, No. 10, 2018, pp. 890–902.

[37] Sierra, M. R., and Coello Coello, C. A., "Improving PSO-Based Multi-objective Optimization Using Crowding, Mutation and ∈-Dominance," *Evolutionary Multi-Criterion Optimization*, edited by C. A. Coello Coello, A. Hernández Aguirre, and E. Zitzler, Springer Berlin Heidelberg, Berlin, Heidelberg, 2005, pp. 505–519. https://doi.org/https://doi.org/10.1007/978-3-540-31880-4_35.

[38] Kennedy, J., and Eberhart, R., "Particle swarm optimization (PSO)," *Proc. IEEE International Conference on Neural Networks, Perth, Australia*, 1995, pp. 1942–1948.

[39] Bogey, C., "Acoustic tones in the near-nozzle region of jets: characteristics and variations between Mach numbers 0.5 and 2," *Journal of Fluid Mechanics*, Vol. 921, 2021, p. A3. https://doi.org/10.1017/jfm.2021.426.

[40] Bogey, C., "Grid sensitivity of flow field and noise of high-Reynolds-number jets computed by large-eddy simulation," *International Journal of Aeroacoustics*, Vol. 17, 2018, pp. 399 – 424. https://doi.org/https://doi.org/10.1177/1475472X18778287.

[41] Bogey, C., and Sabatini, R., "Effects of nozzle-exit boundary-layer profile on the initial shear-layer instability, flow field and noise of subsonic jets," *Journal of Fluid Mechanics*, Vol. 876, 2019, p. 288–325. https://doi.org/10.1017/jfm.2019.546.

[42] Adam, A., Papamoschou, D., and Bogey, C., "Imprint of Vortical Structures on the Near-Field Pressure of a Turbulent Jet," *AIAA Journal*, Vol. 60, No. 3, 2022, pp. 1578–1591. https://doi.org/https://doi.org/10.2514/1.J061010, URL https://doi.org/10.2514/1.J061010.

[43] Michalke, A., and Fuchs, H., "On turbulence and noise of an axisymmetric shear flow," *Journal of Fluid Mechanics*, Vol. 70, No. 1, 1975, pp. 179–205. https://doi.org/10.1017/S0022112075001966.

[44] Huang, C., and Papamoschou, D., *Numerical Study of Noise Shielding by Airframe Structures*, 2008. https://doi.org/10.2514/6.2008-2999.

[45] Morris, P. J., "Jet noise prediction: Past, present and future," *Canadian Acoustics*, Vol. 35, No. 3, 2007, p. 16–22.

[46] Morris, P. J., "A Note on Noise Generation by Large Scale Turbulent Structures in Subsonic and Supersonic Jets," *International Journal of Aeroacoustics*, Vol. 8, No. 4, 2009, pp. 301–315. https://doi.org/10.1260/147547209787548921.

[47] Tam, C. K. W., and Burton, D. E., "Sound generated by instability waves of supersonic flows. Part 2. Axisymmetric jets," *Journal of Fluid Mechanics*, Vol. 138, 1984, p. 273–295. https://doi.org/10.1017/S0022112084000124.

[48] Avital, E. J., Sandham, N. D., and Luo, K. H., "Mach Wave Radiation by Mixing Layers. Part I: Analysis of the Sound Field," *Theoretical and Computational Fluid Dynamics*, Vol. 12, 1998, pp. 73–90. https://doi.org/https://doi.org/10.1007/s001620050100.

[49] Bragge, J., Korhonen, P., Wallenius, H., and Wallenius, J., "Bibliometric Analysis of Multiple Criteria Decision Making/Multiattribute Utility Theory," *Multiple Criteria Decision Making for Sustainable Energy and Transportation Systems*, edited by M. Ehrgott, B. Naujoks, T. J. Stewart, and J. Wallenius, Springer Berlin Heidelberg, Berlin, Heidelberg, 2010, pp. 259–268.

[50] Martins, J. R. R. A., and Ning, A., *Engineering Design Optimization*, Cambridge University Press, 2021. https://doi.org/10.1017/9781108980647.

[51] Coello, C., Pulido, G., and Lechuga, M., "Handling multiple objectives with particle swarm optimization," *IEEE Transactions on Evolutionary Computation*, Vol. 8, No. 3, 2004, pp. 256–279. https://doi.org/10.1109/TEVC.2004.826067.

[52] Zakeri, S., "Ranking based on optimal points multi-criteria decision-making method," *Grey Systems: Theory and Application*, 2018.

[53] Iemma, U., Centracchio, F., and Burghignoli, L., "Aircraft sound quality as Pareto ranking criterion in multi-objective MDO," *INTER-NOISE and NOISE-CON Congress and Conference Proceedings*, Vol. 255, Institute of Noise Control Engineering, 2017, pp. 4946–4955.

[54] Iemma, U., and Centracchio, F., "Sound-Quality-Based Decision Making in Multiobjective Optimisation of Operations for Sustainable Airport Scenarios," *Aerospace*, Vol. 9, No. 6, 2022. https://doi.org/10.3390/aerospace9060310.

[55] Sandham, N., Morfey, C., and Hu, Z., "Sound radiation from exponentially growing and decaying surface waves," *Journal of Sound and Vibration*, Vol. 294, No. 1, 2006, pp. 355–361. https://doi.org/https://doi.org/10.1016/j.jsv.2005.10.012.

[56] Lighthill, M. J., "On sound generated aerodynamically," *General theory. Proc. R. Soc. Lond.*, 1952, pp. 564–587.

[57] Zaman, K., and Yu, J., "Power spectral density of subsonic jet noise," *Journal of Sound and Vibration*, Vol. 98, No. 4, 1985, pp. 519–537. https://doi.org/https://doi.org/10.1016/0022-460X(85)90259-7, URL https://www.sciencedirect.com/science/article/pii/0022460X85902597.

[58] Meloni, S., Di Marco, A., Mancinelli, M., and Camussi, R., "Experimental investigation of jet-induced wall pressure fluctuations over a tangential flat plate at two Reynolds numbers," *Scientific Reports*, Vol. 10, No. 1,1–11, 2020.